



CHORUS

This is the accepted manuscript made available via CHORUS. The article has been published as:

Singlet-Triplet Excitations in the Unconventional Spin-Peierls TiOBr Compound

J. P. Clancy, B. D. Gaulin, C. P. Adams, G. E. Granroth, A. I. Kolesnikov, T. E. Sherline, and F. C. Chou

Phys. Rev. Lett. **106**, 117401 — Published 18 March 2011

DOI: [10.1103/PhysRevLett.106.117401](https://doi.org/10.1103/PhysRevLett.106.117401)

Singlet-Triplet Excitations in the Unconventional Spin-Peierls System TiOBr

J.P. Clancy,¹ B.D. Gaulin,^{1,2,3} C.P. Adams,⁴ G.E. Granroth,⁵ A.I. Kolesnikov,⁵ T.E. Sherline,⁵ and F.C. Chou⁶

¹*Department of Physics and Astronomy, McMaster University, Hamilton, Ontario, L8S 4M1, Canada*

²*Brockhouse Institute for Materials Research, McMaster University, Hamilton, Ontario, L8S 4M1, Canada*

³*Canadian Institute for Advanced Research, 180 Dundas St. W., Toronto, Ontario, M5G 1Z8, Canada*

⁴*Department of Physics, St. Francis Xavier University, Antigonish, Nova Scotia, B2G 2W5, Canada*

⁵*Neutron Scattering Sciences Division, Oak Ridge National Laboratory, Oak Ridge, Tennessee 37831, USA*

⁶*Center for Condensed Matter Sciences, National Taiwan University, Taipei 106, Taiwan.*

We have performed time-of-flight neutron scattering measurements on powder samples of the unconventional spin-Peierls compound TiOBr using the fine-resolution Fermi chopper spectrometer (SEQUOIA) at the SNS. These measurements reveal two branches of magnetic excitations within the commensurate and incommensurate spin-Peierls phases, which we associate with $n = 1$ and $n = 2$ triplet excitations out of the singlet ground state. These results represent the first direct measurement of the singlet-triplet energy gap in TiOBr, which has a value of $E_g = 21.2 \pm 1.0$ meV.

PACS numbers: 78.70.Nx, 75.40.Gb, 75.50.Ee, 75.10.Pq

TiOBr belongs to a select family of quasi-one-dimensional (1D) magnetic materials which undergo a spin-Peierls phase transition. These systems are characterized by a combination of spin 1/2 magnetic moments, short-range antiferromagnetic interactions, and strong magnetoelastic coupling¹. At the spin-Peierls transition temperature, T_{SP} , the quasi-1D spin chains in these systems distort and dimerize, leading to the formation of a non-magnetic singlet ground state. Very few materials have been found to exhibit a spin-Peierls phase transition, and to date there are only three known inorganic spin-Peierls systems: CuGeO₃, TiOCl, and TiOBr.

The isostructural Ti³⁺-based spin-Peierls compounds, TiOCl and TiOBr, have attracted considerable attention as they appear to differ from the standard spin-Peierls scenario in several important respects. TiOCl and TiOBr exhibit not one, but two successive phase transitions upon cooling - a continuous transition from a uniform paramagnetic phase to an incommensurate spin-Peierls state at $T_{C2} \sim 92$ K/48 K, followed by a discontinuous transition into a commensurate spin-Peierls state at $T_{C1} \sim 65$ K/27 K²⁻¹⁴. The TiOX compounds are also distinguished by their unusually high transition temperatures and the surprisingly large energy gap (E_g) between the singlet ground state and the first triplet excited state⁷⁻¹¹. In TiOCl the spin-Peierls state has been shown to be particularly sensitive to the presence of quenched non-magnetic impurities¹⁵.

Experimental studies of these systems have typically focused on TiOCl rather than TiOBr. In practice, this has been the case because TiOBr is extremely hygroscopic and difficult to synthesize in high quality single crystal form. NMR⁷, μ SR⁸, Raman⁹ and IR spectroscopy¹⁰ measurements on TiOCl present a consistent picture of a singlet-triplet energy gap which is between 430 - 440 K. Similar measurements have not been performed for TiOBr, although a gap of ~ 149 K = 12.6 meV has been inferred from low temperature magnetic

susceptibility measurements¹¹. To date, neutron scattering measurements have not been reported for either TiOCl or TiOBr due to the limited size of available single crystal samples. As a result, there is a surprising lack of information regarding the magnetic excitation spectrum of these unconventional spin-Peierls systems.

In this letter we report inelastic neutron scattering measurements on a powder sample of TiOBr. These measurements reveal the magnetic excitation spectrum of this system and provide the first direct measure of the singlet-triplet energy gap. We observe two branches of magnetic excitations, at $\Delta E \sim 21$ meV and $\Delta E \sim 41$ meV, which we associate with $n = 1$ and $n = 2$ triplet excitations out of the singlet ground state. Our measurements show that the bandwidth of these excitations is relatively narrow compared to the size of the energy gap, suggesting that the excitations are well-localized in nature. Furthermore, from the energy scale of the $n = 1$ and $n = 2$ excitations we can infer that the interactions between excited triplets are small.

Time-of-flight neutron scattering measurements were performed on a 2.85 g powder sample of TiOBr. Due to the volatile nature of TiBr₄, the sample was prepared by mixing TiO₂:Ti:TiBr₄ powder in a 2:1:1.4 molar ratio and packing the material in a quartz tube inside a glove box. The packed tubing was removed from the glove box using a valve-controlled transfer tube and was gradually evacuated before flame sealing. The sealed quartz tube was heated at 650 - 700 C for 20 hours, resulting in a final product which was mainly polycrystalline in form.

Neutron scattering measurements were performed using SEQUOIA, the recently commissioned fine-resolution Fermi chopper spectrometer at the Spallation Neutron Source (SNS) at Oak Ridge National Laboratory (ORNL)^{16,17}. SEQUOIA is an ideal instrument for the study of weak magnetic scattering, as it offers a combination of high neutron flux and excellent low-Q detector coverage. Measurements were carried out with Fermi

chopper 2 phased for an incident energy of $E_i = 60$ meV and rotating at a frequency of 480 Hz. This chopper provides ~ 1.5 meV energy resolution at the elastic line under these conditions. A T_0 chopper, used to eliminate unwanted high energy neutrons, was operated at 90 Hz.

The magnetic excitation spectrum of TiOBr is illustrated by the maps of inelastic neutron scattering intensity, $S(Q,E)$, provided in Fig. 1. The magnetic scattering in TiOBr is expected to be quite weak, due to both the small size ($S = 1/2$) and low density (one per formula unit) of the magnetic moments in the system. This problem is exacerbated by the powder nature of the sample, which causes the weak magnetic signal to be averaged over all possible directions in reciprocal space. A further complication arises from the fact that the magnetic excitations in TiOBr occur close in energy to much stronger phonon modes associated with TiOBr and the aluminum sample environment. This combination of factors makes it challenging to isolate the inelastic magnetic scattering in TiOBr, and makes it critical that the experimental background is carefully analyzed and understood.

In general, the scattering observed at any given temperature will consist of three terms: magnetic scattering, phonon scattering, and an approximately temperature independent background term which results from scattering off the sample environment, detector dark current, etc. The background term can effectively be eliminated by performing an empty can background subtraction, leaving only the magnetic and phonon contributions from the sample. The magnetic scattering can then be isolated from the phonon scattering by taking advantage of the different temperature dependencies of the two terms and performing a high temperature background subtraction. At high temperatures, for $T > T_{C2}$, the phonon scattering should dominate the magnetic scattering, and we can make the approximation that:

$$\begin{aligned} I(\omega, T_{high}) &= I_{ph}(\omega, T_{high}) + I_{mag}(\omega, T_{high}) \\ &\approx I_{ph}(\omega, T_{high}) \end{aligned} \quad (1)$$

The low temperature magnetic scattering is then:

$$\begin{aligned} I_{mag}(\omega, T_{low}) &= I(\omega, T_{low}) - I_{ph}(\omega, T_{low}) \\ &= I(\omega, T_{low}) - \left[\frac{1 - e^{(-\hbar\omega/k_B T_{high})}}{1 - e^{(-\hbar\omega/k_B T_{low})}} \right] I(\omega, T_{high}) \end{aligned} \quad (2)$$

The color contour maps provided in Fig. 1 show the inelastic neutron scattering intensity, $S(Q,E)$, for TiOBr at base temperature ($T = 8$ K). At this temperature the system lies well within the commensurate spin-Peierls phase ($T < 27$ K). Fig. 1(a) shows $S(Q,E)$ after an empty can background subtraction has been used to eliminate scattering from the sample environment. Hence 1(a) describes the full scattering contribution from the sample at $T = 8$ K, including both magnetic and phonon terms. Fig. 1(b) shows $S(Q,E)$ after a high temperature (T

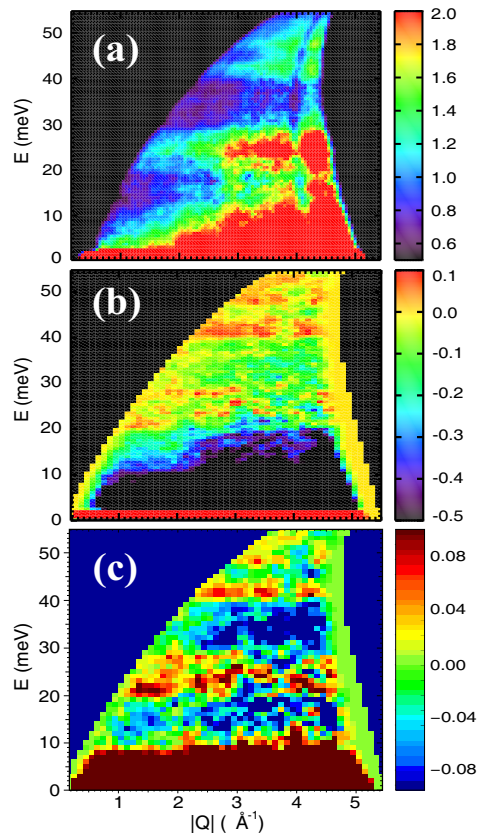


FIG. 1: (Color online) Color contour maps of the inelastic neutron scattering intensity, $S(Q,E)$, for TiOBr at $T = 8$ K (within the commensurate spin-Peierls state). (a) $S(Q,E)$ after an empty can background subtraction to eliminate scattering from the sample environment. (b) $S(Q,E)$ after a high temperature ($T = 80$ K) background subtraction to isolate the magnetic scattering. (c) $S(Q,E)$ after a high temperature background subtraction which has been weighted by an appropriate Bose correction, as described in the text.

$= 80$ K) background subtraction has been used to separate the magnetic scattering from the phonon scattering. Note that because the $T = 80$ K data set lies well within the uniform paramagnetic phase ($T > 48$ K) it is reasonable to assume that the magnetic scattering at this temperature is effectively zero. Fig. 1(c) shows $S(Q,E)$ after a similar high temperature subtraction which has been weighted by an appropriate Bose-correction as described in Eq. 2. In both 1(b) and 1(c) two bands of positive scattering intensity can be observed at energy transfers of ~ 21 meV and ~ 41 meV. These bands represent magnetic excitations, which we associate with the $n = 1$ (one-triplet) and $n = 2$ (two-triplet) excited states, respectively. There are also two regions of negative scattering intensity, from ~ 8 meV to 20 meV and from ~ 28 meV to 40 meV, which we associate with well-defined energy gaps in the excitation spectrum.

Fig. 2 shows a series of cuts through $S(Q,E)$, where

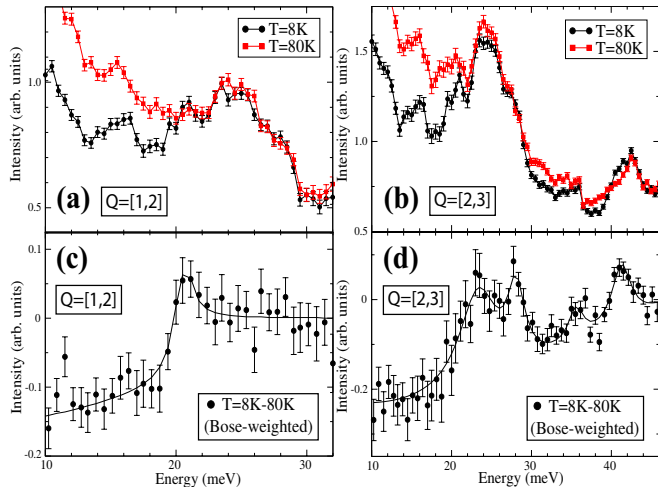


FIG. 2: (Color online) Representative energy cuts through $S(\mathbf{Q}, E)$ at intervals of $|\mathbf{Q}| = 1$ to 2 \AA^{-1} (left) and 2 to 3 \AA^{-1} (right). Panels (a) and (b) provide a direct comparison of the scattering at $T = 8 \text{ K}$ (commensurate spin-Peierls phase) and $T = 80 \text{ K}$ (uniform paramagnetic phase). An empty can background has been subtracted from (a) and (b) in order to eliminate scattering from the sample environment. Panels (c) and (d) show cuts through the $T = 8 \text{ K}$ data set after a Bose-corrected high temperature ($T = 80 \text{ K}$) background has been subtracted in order to isolate the magnetic scattering.

scattering intensity has been integrated over two different regions in \mathbf{Q} -space. \mathbf{Q} -ranges have been chosen to highlight the bottom of the $n = 1$ triplet excitation ($|\mathbf{Q}| = 1$ to 2 \AA^{-1}) and the $n = 2$ triplet excitation ($|\mathbf{Q}| = 2$ to 3 \AA^{-1}). The cuts shown in panels 2(a) and 2(b) were taken through $S(\mathbf{Q}, E)$ after an empty can background subtraction (as employed in Fig. 1(a)). This eliminates scattering from the Al sample can, and in particular the strong Al phonon mode at $\sim 18 \text{ meV}$. The cuts shown in panels 2(c) and 2(d) were taken through $S(\mathbf{Q}, E)$ after a Bose-weighted high temperature ($T = 80 \text{ K}$) background subtraction (as employed in Fig. 1(c)). As a result, the scattering in 2(c) and 2(d) should be strictly magnetic in origin. Note that there is only one magnetic peak in the low- \mathbf{Q} cut shown in 2(c), while there appear to be several additional peaks in the higher- \mathbf{Q} cut provided in 2(d). The \mathbf{Q} -dependence of these additional peaks suggests they may be phonon-like rather than magnetic in nature, potentially reflecting small temperature dependent changes in the phonon density of states. Alternatively, these peaks may simply reflect the powder-averaged dispersion of the magnetic excitations. The solid lines provided in 2(c) and 2(d) represent fits to the data performed using multiple Lorentzian lineshapes.

The magnitude of the singlet-triplet energy gap in TiOBr is defined by the lower bound of the $n = 1$ triplet excitation. Thus, by fitting the data in Fig. 2 we obtain a value of $E_g = 21.2 \pm 1.0 \text{ meV} \sim 250 \text{ K}$. This value is

significantly higher than the reported value of 12.6 meV inferred from magnetic susceptibility measurements¹¹. However, our experimental value of E_g is remarkably consistent with previous measurements of the singlet-triplet energy gap in TiOCl⁷⁻¹⁰. By starting from the reported value of $E_{\text{TiOCl}} = 430 - 440 \text{ K}$, and scaling by the ratio of the exchange couplings determined from magnetic susceptibility ($J_{\text{TiOCl}} = 660 - 676 \text{ K}^2$,¹² and $J_{\text{TiOBr}} = 364 - 376 \text{ K}^2$,¹¹⁻¹⁴) one obtains a prediction of $E_{\text{TiOBr}} = \left(\frac{J_{\text{TiOBr}}}{J_{\text{TiOCl}}} \right) \times E_{\text{TiOCl}} = 19.6 - 21.3 \text{ meV}$, in excellent agreement with our experimental results.

As in the case of TiOCl, this value of E_g is unusually large compared to both the size of the gap in other spin-Peierls systems ($E_{\text{CuGeO}_3} = 2.1 \text{ meV}$ ^{18,19}) and the size of the energy scale determined by T_{C1} and T_{C2} . The BCS prediction for E_g in a conventional spin-Peierls system yields a value of $\frac{2E_g}{k_B T_{SP}} \sim 3.5$ ¹. While this prediction is almost perfectly realized in the case of CuGeO₃ ($\frac{2E_g}{k_B T_{SP}} = 3.54$ ^{18,19}), it appears to provide a poor description of the energy gap in the Ti-based spin-Peierls compounds ($\frac{2E_g}{k_B T_{SP}} \sim 10$ to 13 in TiOCl and 10 to 18 in TiOBr).

It is interesting to note that the energy scale for the $n = 2$ triplet excitation is almost exactly twice the energy scale of the $n = 1$ triplet excitation. This implies that the interactions between excited triplets must be small, as any inter-triplet coupling should act to shift the $n = 2$ excitation away from $\Delta E = 2E_g$. A similar result has been observed in CuGeO₃, where inelastic neutron scattering measurements reveal well-defined $n = 1$ triplet excitations at $\sim 2.1 \text{ meV}$ which are separated from a continuum of states by a second, approximately equal, energy gap of $\sim 2 \text{ meV}$ ^{20,21}. This may be contrasted with other singlet ground state systems, such as the Shastry-Sutherland system SrCu₂(BO₃)₂, in which the interactions between triplets are much stronger. In SrCu₂(BO₃)₂, these interactions reduce the energy of the $n = 2$ excitation by $\sim 40 \%$, giving rise to $n = 1$ and $n = 2$ features at $\sim 3 \text{ meV}$ and 4.9 meV , respectively^{22,23}.

While it is difficult to determine a precise bandwidth for the magnetic excitations in TiOBr, it is reasonable to place an upper bound of $\sim 8 \text{ meV}$ on the $n = 1$ excitation, which extends at most from 20 meV to 28 meV . This bandwidth is relatively small compared to the size of the singlet-triplet energy gap ($\sim 40 \%$ of E_g), suggesting that the excited triplets are fairly well-localized. This represents a significant difference from the excitation spectrum of CuGeO₃, in which the dispersion ranges from $\sim 25 \%$ (inter-chain) to $\sim 800 \%$ (intra-chain) of E_g ^{19,20}. In part, the magnetic excitations in TiOBr may be less dispersive because of the geometric frustration inherent to the buckled Ti-O bilayer crystal structure. Certainly geometric frustration is believed to be responsible for the largely dispersionless singlet-triplet excitations observed in SrCu₂(BO₃)₂^{22,23}.

The temperature dependence of the magnetic excita-

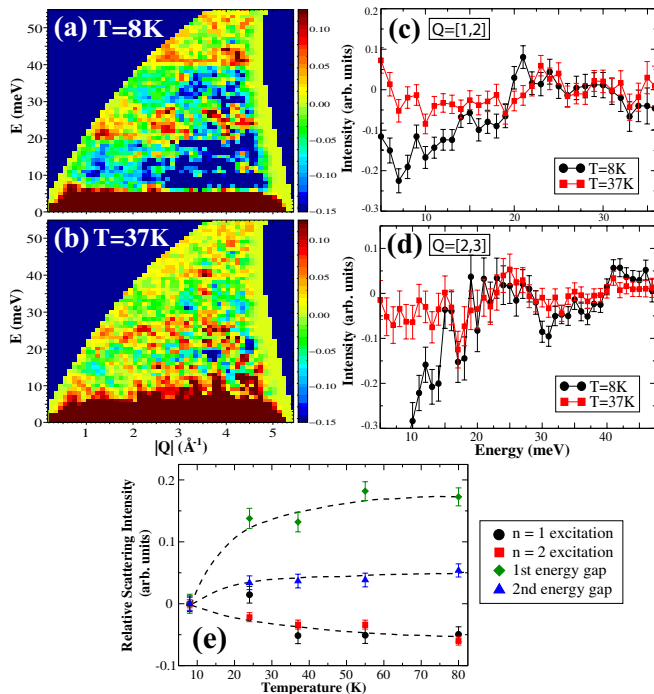


FIG. 3: (Color online) Temperature dependence of magnetic excitations in TiOBr. Color contour maps of the inelastic scattering intensity, $S(Q,E)$, are shown for (a) $T = 8\text{ K}$ (commensurate spin-Peierls phase) and (b) $T = 37\text{ K}$ (incommensurate spin-Peierls phase). A Bose-corrected high temperature ($T = 55\text{ K}$) background has been subtracted from (a) and (b) in order to isolate the magnetic scattering. Representative energy cuts through (a) and (b) are provided for (c) $Q = [1, 2]\text{ \AA}^{-1}$ and (d) $Q = [2, 3]\text{ \AA}^{-1}$. The integrated scattering intensity of the $n = 1$ and $n = 2$ triplet excitations and the first and second energy gaps is shown in (e). All intensities are expressed relative to the scattering observed at $T = 8\text{ K}$, and all dashed lines are provided as guides-to-the-eye. Ranges of integration are described in the main text.

tion spectrum in TiOBr is illustrated by Fig. 3. Figs. 3(a) and 3(b) provide color contour maps of $S(Q,E)$ in the commensurate ($T = 8\text{ K}$) and incommensurate ($T = 37\text{ K}$) spin-Peierls states after a Bose-weighted high temperature ($T = 55\text{ K}$) background subtraction. While two branches of magnetic excitations can be observed in both low temperature phases, there are clear differences between the magnetic scattering at $T = 8\text{ K}$ and $T = 37\text{ K}$. In particular, both the $n = 1$ and $n = 2$ triplet

excitations appear to be weaker in the incommensurate spin-Peierls state, and both the first and second energy gaps appear to have partially filled in by $T = 37\text{ K}$. These effects are also visible in the representative energy cuts provided in Figs. 3(c) and 3(d).

Fig. 3(e) describes the temperature evolution of the inelastic scattering intensity at energies corresponding to the $n = 1$ and $n = 2$ triplet excitations and the first and second energy gaps. Integrated intensities were obtained by binning up scattering intensity over ranges of: $Q = 1$ to 2 \AA^{-1} and $E = 20$ to 22 meV ($n = 1$ triplet), $Q = 2$ to 3 \AA^{-1} and $E = 40$ to 42 meV ($n = 2$ triplet), $Q = 1$ to 3 \AA^{-1} and $E = 10$ to 12 meV (first energy gap), and $Q = 1$ to 3 \AA^{-1} and $E = 30$ to 32 meV (second energy gap). The intensities in 3(e) have been normalized by appropriate Bose-factors in order to account for thermal population effects. For illustrative purposes, all intensities have been expressed relative to the scattering at $T = 8\text{ K}$, at which point both the magnetic excitations and the singlet-triplet energy gap are assumed to be fully developed. The temperature dependence of the data clearly supports our interpretation of these four features, as the intensity of the $n = 1$ and $n = 2$ excitations gradually drops with increasing temperature, and the intensity within the two energy gaps steadily rises.

In conclusion, we have observed two branches of magnetic excitations in the commensurate and incommensurate spin-Peierls phases of TiOBr, which can be understood as $n = 1$ and $n = 2$ triplet excitations out of the singlet ground state. The singlet-triplet energy gap is found to be $E_g = 21.2 \pm 1.0\text{ meV}$, a result which is dramatically larger than the standard BCS prediction, but which is fully consistent with the anomalously large gap reported for TiOCl ⁷⁻¹⁰. The magnetic excitations in TiOBr exhibit relatively little dispersion, and are consistent with well-localized and weakly interacting excited triplets. We hope these results will help to guide and inform future studies of these novel magnetic systems.

The authors would like to acknowledge S. H. Huang for sample preparation, and C. Stock, A. Aczel, and J.P.C. Ruff for helpful discussions. This work was supported by NSERC of Canada and NSC of Taiwan under project No. NSC-98-2119-M-002-021. Research at the SNS at ORNL was sponsored by the Scientific User Facilities Division, Office of Basic Energy Sciences, U.S. Dept. of Energy. ORNL is managed by UT-Batelle, LLC, under contract DE-AC0500OR22725 for the U.S. Dept. of Energy.

¹ J.W. Bray et al. in *Extended Linear Chain Compounds*, edited by J.S. Miller (Plenum Press, New York, 1983), Vol. 3, p. 353.

² A. Seidel et al., Phys. Rev. B **67**, 020405(R) (2003).

³ P. Lemmens et al., New J. Phys. **7**, 74 (2005).

⁴ S. van Smaalen et al., Phys. Rev. B **72**, 020105(R) (2005).

⁵ J.P. Clancy et al., Phys. Rev. B **75**, 100401(R) (2007).

⁶ J.P. Clancy et al., Phys. Rev. B **81**, 024411 (2010).

⁷ T. Imai and F.C. Chou, arXiv:cond-mat/0301425v1 (unpublished); S.R. Saha et al., J. Phys. Chem. Solids **68**, 2044 (2007).

⁸ P.J. Baker et al., Phys. Rev. B **75**, 094404 (2007).

- ⁹ P. Lemmens et al., Phys. Rev. B **70**, 134429 (2004).
- ¹⁰ G. Caimi et al., Phys. Rev. B **69**, 125108 (2004).
- ¹¹ T. Sasaki et al., arXiv:cond-mat/0501691v2 (unpublished).
- ¹² R. Ruckamp et al., Phys. Rev. Lett. **95**, 097203 (2005).
- ¹³ C. Kato et al., J. Phys. Soc. Jpn. **74**, 473 (2005).
- ¹⁴ T. Sasaki et al., J. Phys. Soc. Jpn. **74**, 2185 (2005).
- ¹⁵ J.P. Clancy et al., Phys. Rev. B **78**, 014433 (2008).
- ¹⁶ G.E. Granroth et al., Physica B **385-386**, 1104 (2006).
- ¹⁷ G.E. Granroth et al., J. Phys.: Conf. Ser. **251**, 012058 (2010).
- ¹⁸ M. Nishi et al., Phys. Rev. B **50**, 6508 (1994).
- ¹⁹ L.P. Regnault et al., Phys. Rev. B **53**, 5579 (1996).
- ²⁰ M. Arai et al., Phys. Rev. Lett **77**, 3649 (1996).
- ²¹ M. Ain et al., Phys. Rev. Lett. **78**, 1560 (1997).
- ²² B.D. Gaulin et al., Phys. Rev. Lett. **93**, 267202 (2004).
- ²³ H. Kageyama et al., Phys. Rev. Lett. **84**, 5876 (2000).